Food Chemistry xxx (xxxx) xxxx

Contents lists available at ScienceDirect

Food Chemistry

journal homepage: www.elsevier.com/locate/foodchem

Understanding the role of atmospheric cold plasma (ACP) in maintaining the quality of hairtail (*Trichiurus Lepturus*)

John Kilian Koddy[a,1], Wenhua Miao[a,1,*], Shaimaa Hatab[b,c,*], Lingling Tang[a], Huiqian Xu[a], Bhoke Marwa Nyaisaba[a], Meiling Chen[a], Shanggui Deng[a]

[a] Department of Food Science and Pharmaceutics, Zhejiang Ocean University, 316022 Zhoushan, China
[b] Faculty of Environmental Agricultural Science, Arish University, 45516 North Sinai, Egypt
[c] Faculty of Organic Agriculture, Heliopolis University, 2834 Cairo, Egypt

ARTICLE INFO

Keywords:
Endogenous enzyme activity
Cold atmospheric plasma
Texture profile
Color properties
Water holding capacity
Protein oxidation

ABSTRACT

Impacts of atmospheric cold plasma (ACP) on the properties of muscle protein and performance of extracted crude enzyme of hairtail (*Trichiurus Lepturus*) fish have been evaluated. A decrease in extracted crude enzyme activity with increasing the ACP treatment time has been found, and the highest reduction ($p < 0.05$) value of 0.035 units/mg proteins was obtained after 240 s. A considerable increase in the carbonyl content in the treated sample for about three times higher than the control sample was found, and a decrease of total sulfhydryl content to 0.34 nmol/mg protein. Texture profile analysis, water holding capacity, and the color properties of the muscle protein improved significantly in the samples treated with ACP. SDS-PAGE pattern showed an increase in the band intensity of cross-linked myosin heavy chains and actin proteins. Based on these outcomes, ACP could play a significant role as a promising non-thermal method to prolong the shelf-life of hairtail fish.

1. Introduction

Hairtail (*Trichiurus lepturus*) fish is a common benthopelagic commercial marine fish in the eastern Pacific Ocean. Appealing flavor, taste, as well as the high nutritional value of Hairtail, make it one of most mainstream fish on the Chinese table (Luan, Sun, Chen, Wu, & Hu, 2018). However, the sensitivity of hairtail to perish is more than other marine fish species due to its high content of unsaturated fatty acids that affect nutritional value, color, and flavor negatively (Luan et al., 2018). To prolong fish shelf-life and maintain the quality, different preservation methods have been utilized most of them depend on using low temperatures including chilling (0–4 °C), superchilling (−1 to −3 °C), and freezing (−18, −20 °C) (Luan et al., 2017, 2018). The shelf-life of chilled fish is limited, where the action of enzymes and bacteria under chilling temperature can be slowed down but cannot be inhibited (Fernández, Aspé, & Roeckel, 2010). During the frozen storage of fish undesirable breakdown of the quality could happen including unwanted texture and flavor changes, crystallization, lipid oxidation, water loss, and tissue dehydration (Luan et al., 2017). With increasing consumer demand for fish consumption as well to reduce the economic losses, the development of new and efficient preservation methods for fish is highly required. The consumer assessment of fish freshness depends mainly on several parameters including water-holding capacity, appearance, odor, texture, drip loss or cook loss, and pH value. As far as we know, the use of non-thermal processes as a potential conservation method for such perishable products is not well studied yet.

An eco-friendly, highly efficient, and non-thermal technology called Atmospheric cold plasma (ACP) has been developed. ACP has been extensively utilized to improve food products by endogenous enzymes inactivation, modifications of food packaging condition, microbial decontamination, and toxin removal (Pankaj, Wan, & Keener, 2018). From a food processing perspective, the major advantages of ACP compared to the traditional thermal processes are the maintenance of the product overall quality, sensory attributes, and nutritional value. On this basis, several studies carried out to conclude the impact of plasma species on deleterious enzymes especially those causing protein decomposition resulting in hinders the production of high-quality food with a long shelf life (Gavahian, Chu, & Jo, 2019; Segat, Misra, Cullen, & Innocente, 2016; Zhang et al., 2015). Yet, no detailed description is available about the action of ACP on endogenous enzymes and thus the quality of hairtail fish. In order to provide a better understanding of

* Corresponding authors at: Faculty of Environmental Agricultural Science, Arish University, 45516 North Sinai, Egypt and Faculty of Organic Agriculture, Heliopolis University, 2834 Cairo, Egypt (S. Hatab).
E-mail addresses: miaowenhua@126.com (W. Miao), shimaa.reda@hu.edu.eg (S. Hatab).
[1] These authors contributed equally to this work.

https://doi.org/10.1016/j.foodchem.2020.128418
Received 24 June 2020; Received in revised form 14 October 2020; Accepted 14 October 2020

plasma interactions with muscle proteins, this research focused basically on the impact of ACP on the quality and physicochemical properties of hairtail protein. Different complementary methodologies including water holding capacity, carbonyl content, total sulfhydryl content, solubility, turbidity, texture properties, color, endogenous enzyme activity as well as gel electrophoresis (SDS-PAGE) have been undertaken to assess the impact of ACP on hairtail. To identify the optimum time for implementing ACP, different treatment times (30, 60, 120, 180, 240, 300 s) have been considered.

2. Materials and methods

2.1. Materials

Twenty kg of frozen hairtail (*Trichiurus lepturus*) fish was purchased from the local market in Zhoushan, Zhejiang Province, China. An icebox has been used to transfer the fish samples to the laboratory directly. Upon arrival, the samples were cut into pieces then stored at −80°C to prevent further protein degradation. Analytical grade reagents including TrisBase, hydrochloric acid (HCl), Nalpha-benzoyl-L-argininamide hydrochloride monohydrate, Trichloroacetic acid (TCA), 2, 4-dinitrophenylhydrazine, L-Tyrosine, Monosodium dihydrogen sulfate, Disodium monohydrogen phosphate, Bovine Serum Albumin (BSA) sodium hydroxide, 5, 5-dithiobis (2-nitrobenzoic acid) – DTNB, mercaptoethanol, EDTA (ethylenediaminetetraacetic acid), sample and running buffers, Coomassie Brilliant Blue (BlueTM SafeStain) and protein standards (MarkPR1910) applied for SDS-PAGE were purchased from Solar bio Science & Technology Co., Ltd (Beijing, China). Sinopharm Chemical Reagent Co. Ltd provided us with the other used reagents (Shanghai, China).

2.2. Crude protease extract (CPE)

Crude protease extract (CPE) was utilized as an indicator to assess the performance of the endogenous enzyme. Crude protease enzyme has been extracted from hairtail flesh as described by Ketnawa, Martinez-Alvarez, Benjakul, and Rawdkuen (2015) after adjustments (Ketnawa et al., 2015). Briefly, the stored samples (-80 °C) were allowed to thaw, and then deskinned, deboned, and afterward cut into small pieces of approximately 1 – 1.5 cm. After that, the samples were mixed with [10 mM Tris–HCl (pH 8.0)] buffer, containing 10 mM $CaCl_2$] at a ratio of 1:5 (w/v), and then homogenized for 2 min using a high-speed blender (VM0109, Vita-Mix Corporation, Cleveland, USA). A Hitachi Himac CF 16 RX (Tokyo, Japan) has been used to centrifuge the suspension at 4 °C and 10000 rpm for 10 min. The supernatant which refers to the crude protease extract (CPE) has been collected.

2.3. Atmospheric cold plasma (ACP) treatment

The plasma generating instrument used in this study was the Dielectric Barrier Discharge (DBD) (AC Test Set, 600 series, model number BK130/36, Phenix Technologies, Inc. USA) as described earlier by Nyaisaba et al. (2019). The DBD plasma source was made up of two parallel rounded aluminum plates with an outer diameter of 155 mm and had a distance of 75 mm between the two electrodes. In each end, dielectric barriers of polystyrene boards (2 mm thickness) separated both the sample and the electrodes. A high voltage transformer was used to provide the energy required to generate the reactive oxidative plasma species from atmospheric gas. For sample treatments, 10 mL of crude protease extract with 89 mm diameter and 2 mm thickness were put into Petri dishes. The samples have been treated with a voltage of 50 kV for 30, 60, 120, 180, 240, and 300 s. Samples without ACP treatment was also included as a control.

Moreover, 25 g of hairtail muscle samples were placed in Petri dishes with a diameter of 100 mm and thickness of 15 mm and subjected to a voltage of 50 kV for 30, 60, 120, 180, 240, and 300 s intervals. Untreated hairtail muscles were included and used as control samples.

2.4. Determination of the effect of ACP on temperature and pH value

The effect of atmospheric cold plasma (ACP) on the initial temperature and pH value of CPE has been assayed as described by Nyaisaba et al. (2019). pH meter (Sartorius PB-10) has been used to measure initial pH value before and after ACP treatment. As well, the temperature of CPE was measured using a normal thermometer before and immediately after ACP treatment.

2.5. Determination of proteolytic enzymatic activity

Tyrosine has been used as a standard to determine the proteolytic enzymatic activity as conducted by Nyaisaba et al. (2019). Briefly, 200 μL of CPE treated with ACP (at 50 kV) for different times was mixed with 2 mg of the substrate (Nalpha-benzoyl-L-argininamide hydrochloride monohydrate), 200 μL of distilled water, and 625 μL reaction buffers (10 mM Tris–HCl (pH 8.0), containing 10 mM $CaCl_2$). After properly mixing, the solution incubated for 30 min at 37 °C. After incubation, the enzymatic reaction was terminated by adding 200 μL of 5% (w/v) cold Trichloroacetic acid (TCA), then kept at 4 °C for 1 h to allow the unhydrolyzed protein substrate to precipitate. The mixture was centrifuged at 5000 rpm for 10 min at 4 °C, afterword the absorbance has been recorded at 750 nm using Hitachi U-2000 UV–Vis spectrophotometer (Tokyo, Japan). The endogenous enzyme activity was determined by measuring the amount of tyrosine released per gram of protein (μmole Tyr g^{-1} protein). The same method has been used with the blank sample except that the CPE was added after addition of 5% TCA. Three replicates were performed for each treatment.

2.6. Investigating the impact of pH and temperature on crude protease activity

The effect of temperature and pH on crude proteolytic enzyme activity was determined as described by Klomklao, Benjakul, Kishimura, and Chaijan (2011). The optimum temperature for enzyme activity was determined by incubating the samples after ACP treatment at different temperatures (25, 35, 45, 55, 65, 75, and 85 °C) under the optimum pH for 10 min using a temperature-controlled water bath. After incubation, the samples were immediately cooled in iced water. For pH profile, the activity was determined under different pH (2.4, 3.0, 4.0, 5.0, 6.0, 7.0, and 8.0) at 37 °C for 20 min. McIlvaine's buffer (0.2 mmol/L disodium phosphate and 0.1 mol/L citric acid) has been used. Nalpha-benzoyl-L-argininamide hydrochloride monohydrate has been used as a substrate to assay the residual activity of the crud protease (CP) at various temperatures and pH (Benjakul & Visessanguan, 2003).

2.7. Determination of carbonyl content

The carbon content was estimated by incubating with 2,4-dinitrophenylhydrazine (DNPH, Sigma-Aldrich, USA) as given by Chen, Zhou, and Zhang (2015) with slight modifications. CPE after ACP treatment was precipitated with 10 mM Tris-HCl buffer (pH 8.0) at a ratio of 1:5 (v/v). Then 400 μL of the sample were separated into two different tubes coded sample tube (S) and control tube (C). Eighty μL of 50% TCA was added to each tube. The tubes were centrifuged for 3 min at 4 °C and 12,000 rpm. The pellets were collected and mixed with 500 μL 0.2% of 2, 4-dinitrophenylhydrazine (DNPH) in 2 M HCl followed by incubation in a dark place at room temperature for 60 min with regulating shaken every 15 min. The precipitate was purified with 0.5 mL of 10% TCA and centrifuged again after 5 min incubation at 4 °C. One mL ethanol: ethyl acetate (1:1 v/v) was used to wash the precipitates twice. Finally, the precipitates were dissolved in 1.5 mL of 6 M guanidine hydrochloride dissolved in 20 mM sodium phosphate

buffer (pH 6.5) then centrifuged to remove any remaining debris in the supernatant. The sample absorbance was read at 365 nm using Hitachi U-2000 UV–Vis spectrophotometer (Tokyo, Japan). The actual extinction coefficient for dinitrophenyl hydrazine calculated at 370 nm using standard bovine serum albumin (BSA) in guanidine solution. The absorption coefficient of 22,000 $M^{-1}cm^{-1}$ was used for protein hydrazine.

2.8. Determination of total sulfhydryl content

One mL of CPE after ACP treatment was added to 8 mL of dissociating buffer (5.2 g Tris-HCl, 3.45 g glycine, 240 g urea, 0.6 g EDTA all in 500 mL distilled water pH 8.0) and 0.5 mL of Ellman's reagent (4 mg./mL 5,5-dithiobis (2-nitrobenzoic acid) DTNB. The resulting solution was incubated at room temperature in a dark place for 30 min. Afterward, the absorbance of samples was measured at 412 nm using Hitachi U-2000 UV–Vis spectrophotometer. The molar absorbance coefficient of 13,600 $M^{-1}L^{-1}cm^{-1}$ was used to calculate SH concentration in samples. The final results are expressed as nanomoles of total sulfhydryl per mg of protein (Li, Kong, Xia, Liu, & Diao, 2013).

2.9. Preparation of hairtail muscle protein concentrate

The total protein was extracted from 1 g minced muscle of hairtail using 10 mM Tris-HCl buffer solution pH 8.0 (containing 10 mM $CaCl_2$) at a ratio of 1:2 (w/v) and homogenized in a blender at low speed for 2 min (Ketnawa et al., 2015). The homogenate was centrifuged at 5,000 rpm for 15 min at 4 °C. The supernatant was discarded and the precipitate was considered as protein concentrates.

2.10. Determination of protein solubility and turbidity

The turbidity of hairtail protein after ACP treatment was obtained by measuring the absorbance of the solutions using a UV–Vis spectrophotometer at 350 nm. Protein solubility was measured using the biuret method, according to the method of (Nyaisaba et al., 2019) with some modifications. After ACP treatment, one mL of supernatant was mixed with 4 mL of biuret reagent then vortex mixed. The mixture was incubated at room temperature (37 °C) for 30 min and absorbances were read at 540 nm using Hitachi U-2000 UV–Vis spectrophotometer (Tokyo, Japan). The protein solubility was expressed as dissolved protein content in the supernatant to the total protein content of the sample, as follows:

$$\text{Protein solubility (\%)} = \frac{\text{Supernatant protein content}}{\text{Sample protein content}} \times 100 \quad (1)$$

2.11. Texture profile analysis (TPA)

Texture profile analysis (TPA) of hairtail protein was measured using a texture analyzer (TMS-Pro, Food Technology, Inc.). Protein concentrated samples were compressed to 30% of its initial thickness using a cylindrical plunger having a 50 mm diameter, with a trigger force of 0.6 N and a pressing at a constant speed of 60 mm/min. The force–time results curves for TPA, including hardness (N), cohesiveness, springiness, and adhesiveness (μJ) were obtained. The evaluation involved the mean value of three replicates (Benjakul & Visessanguan, 2003)

2.12. Determination of water holding capacity (WHC)

Water holding capacity (WHC) of hairtail protein samples were determined using weight loss as described by Benjakul andVisessanguan (2003) with minor modifications. About 5 g of hairtail protein concentrates were cut and weighed accurately (W_1) then placed between three layers of Whatman paper No.1 and subsequently loaded into 50 mL centrifuge tubes, then centrifuged at 5000 rpm for 10 min at 4 °C. The samples were then removed from the paper and re-weighed (W_2). The WHC of the samples was then calculated and expressed as a percentage of sample weight as follows:

$$\text{WHC (\%)} = \frac{W_1}{W_2} \times 100 \quad (2)$$

2.13. Measurement of muscle protein color

The Minolta Chroma Meter CR-400/410 colorimeter was used to analyze the color of the hairtail protein. The color parameters L^* (lightness), a^* (red/green) and b^* (yellow/blue) were measured. A light trap and a white calibration plate were used to standardize a calorimeter. Measurements were taken at three different points on each tested sample.

2.14. Electrophoresis

Detection of the protein patterns in hairtail muscle concentrate was done using Sodium dodecyl sulfate–polyacrylamide gel electrophoresis (SDS-PAGE) (Nyaisaba et al., 2019). Briefly, six μl of the aliquot sample was obtained after diluting sample solution with protein buffer at a ratio of 1:3 and 5 μL of protein marker PR1910 (11KDa – 180 kDa) (Solar bio Science & Technology Co., Ltd Beijing, China) were injected in the wells. In the beginning, the system allowed to run at 80 V until the sample and protein marker aligned then the power was re-set to 120 V and allowed to run for 1 h. After separation, the gel was stained for 2 h in 0.1% (w/v) Coomassie Brilliant Blue R-250 in 50% (v/v) methanol and 7.5% (v/v) acetic acid then decolorized in deionized water containing 7.5% (v/v) acetic acid and 5% (v/v) methanol. Staining and decolonization processes were done at a slow speed moving shaker. Molecular weight (MW) of each protein bands were estimated using a distance of protein migration in comparison to the MW of the protein marker.

2.15. Statistical analysis

All analyses were performed in triplicate and the data presented are the mean ± S.D. Statistical data analysis was performed using originPro software (Version 8.0 Microcal Software Inc., Northampton, MA) and SPSS software (IBM statistical analysis Version 20) to indicate a statistical significance level at $p < 0.05$. A one-way analysis of variance (ANOVA) was used to find statistical differences existed between control and treated samples. Significance differences between sample means were identified using Duncan's multiple range tests at a significance level of $p < 0.05$ (Miao et al., 2020).

3. Results and discussion

Proteins are the basic material of tissue structure. They represent about 80% of dry mass in lean tissue and 20% of the total muscle weight (Ekezie, Cheng, & Sun, 2019). Any changes that occur in hairtail protein would contribute to the final quality of the meat. Since protease is the main responsible for the degradation of myofibril protein, which leads to undesirable changes in the meat texture properties (Cheng & Sun, 2008). Particularly, protease influences hydrophobic properties and the molecular weight of proteins and as a result, the protein functional properties affected (Shavandi, Hou, Carne, McConnell, & Bekhit, 2019). Therefore, the effect of ACP on the physicochemical properties and structural changes in crude protease extract from hairtail fish have been investigated in the present study.

3.1. Temperature and pH profile of crude protease activity

The results indicated that the ACP could cause a slight increase in

the initials temperature of CPE as well as the pH (see supplementary data Table A). The insignificant shift in the temperature and pH might be attributed to the reactive plasma species imparted in the samples by ACP. The initial pH of CPE was 6.73 ± 0.25. A gradual decrease in pH was found to reach 6.67 ± 0.15 in the samples submitted to 50 kV at 300 s. It has been found that the pH of liquid matrices could be reduced by plasma species (Ekezie et al., 2019; Segat, Misra, Cullen, & Innocente, 2015). Graves (2014) figure out that the acidification in the air plasma is expected due to the production of nitrous acid (HNO_2) and nitric acid (HNO_3) which have acidifying and oxidizing effects (Graves, 2014).

Changes in temperature of different treatments showed a similar trend in which a slight increase was observed in different degrees (see supplementary data Table A). This result was in accordance with the findings obtained by Nyaisaba et al. (2019) who found an increase in crude protease extracts' temperature from squid to be about 28oC after cold atmospheric plasma treatment (Nyaisaba et al., 2019). The highest temperature reported in this study was 28.20 ± 0.29 after treating by ACP for 180 and 240 s. this temperature is insufficient to inhibit the activity of crude enzyme extract in the treated samples.

3.2. Effect of ACP on proteolytic enzymatic activity

The consumer acceptability and the market price of fish depend mainly on the texture of the fish. Therefore, the mushy or soft texture of fish is unfavorable and limits its shelf-life. One of the main reasons for that is the presence of active proteases in digestive organs and muscle, that cause significant degradation of myofibrillar and collagenous proteins (Singh & Benjakul, 2018). ACP was found to have a significant impact on the peroxidase (POD) inactivation in tomato (Pankaj, Misra, & Cullen, 2013) as well as oxidase (PPO) in the apple (Tappi et al., 2014), and thus retard the undesirable changes during storage. To lower muscle degradation, the effect of ACP on the activity of crude protease extract has been investigated.

The results showed that the inactivation of crude protease extract by ACP is affected by plasma species and exposure time (Fig. 1.). A significant decrease in the enzyme activity has been observed with increasing the treatment time (Fig. 1), where the lowest enzyme activity value of 0.035 units/mg was recorded after 240 s of treatment. This probably due to the interaction between plasma species and protein polymers which results in changes in the molecule structure of the protein (Segat et al., 2016). Our findings consistent with Nyaisaba et al. (2019) and Zhang et al. (2015) who indicated that ACP treatment time is significantly affected the changes induced in the protein structure (Nyaisaba et al., 2019; Zhang, Xue, Li, Wang, & Xue, 2015). What is more, the DBD set-up is capable of generating considerable amounts of ozone and hydrogen peroxide, that contribute to the rapid inactivation of the enzyme (Segat et al., 2016). That happens through the chemical interaction between the amino acids side-chains and hydroperoxyl radicals (HOO^-), superoxide anion radicals (O_2^-), nitric oxide (NO), and hydroxyl radicals (OH) induce structural changes of the enzyme (Pankaj et al., 2013). In this context, Zhang et al. (2015) found that the reactive plasma species produced by DBD were able to inactivate Lactase Dehydrogenase (LDH) enzyme, which is responsible for instigating protein denaturation (Zhang et al., 2015).

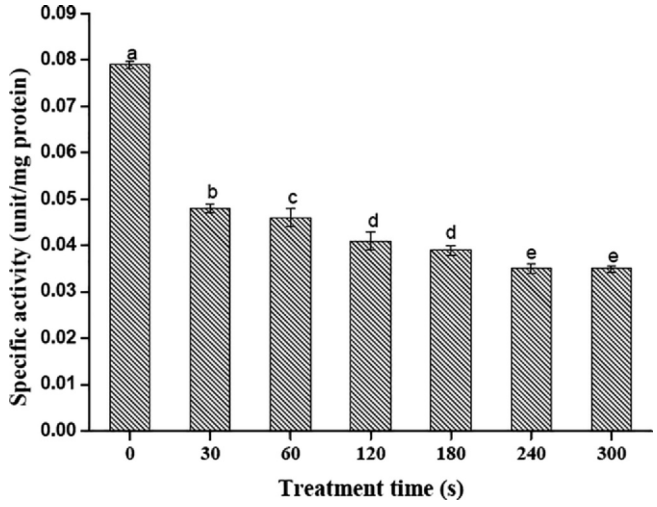

Fig. 1. Effect of atmospheric cold plasma (ACP) on proteolytic enzymatic. Data are presented as mean ± standard deviation (n = 3). 0 s refers to the untreated sample (control). Different letters on top of bars indicate a statistically significant difference at $p < 0.05$.

3.3. Effect of temperature and pH on the crude protease activity

The effects of temperature and pH on the activity of crude protease extracts were conducted to give an overview of the optimum conditions for the performance of the proteolytic enzyme in hairtail fish muscles. Crude protease from hairtail muscle showed the highest activity (0.067 units/mg) at 45 °C, with the increasing temperature a sharp decrease in the enzyme activity was obtained (see supplementary data Fig. B). The decrease in the enzyme activity probably due to denaturation caused by high temperatures. The proteolytic activity temperature ranges between 25 and 75 °C, while the optimum activity occurs between 40 and 50 °C (Gómez-Guillén, Hurtado, & Montero, 2002). These results correlate favorably with other studies conducted on squid protease, where it was found that the maximum proteolytic activity was attained at 50 °C (Nyaisaba et al., 2019) and 40 °C (Konno & Fukazawa, 1993) then decreased at high temperatures.

For pH profile, it was noted that the maximum enzymatic activity of 0.058 units/mg was obtained at pH 3, and slight enzyme activity of 0.044 units/mg protein was observed at pH 7 (see supplementary data Fig. B). This confirms previous findings in the literature, where the highest activity of crude protease extract was noted at pH 3 and 7 (Nyaisaba et al., 2019). To avoid undesirable effects during the storage and processing of hairtail fish, our findings identify the temperature and pH which could be implemented to deactivate the protease, limit softening, and enhance the final quality of the product.

3.4. Effect of ACP on sulfhydryl and carbonyl contents

Sulfhydryl carbonyl content of the treated sample has been measured to identify the ability of ACP to oxidize the crude protease extract. In general, Oxidation of proteins modifies the amino acid side-chains and changes in the protein polypeptide backbone, resulting in protein fragmentation, cross-linking, conformational and unfolding changes (Stadtman, 2006; Zhang, Xiao, & Ahn, 2013). These structural changes negatively affect the protein function including enzyme activity (Zhang et al., 2013).

The results indicate that the sulfhydryl content (SH) was significantly affected by ACP treatment, where the SH content decreased ($P < 0.05$) as the ACP treatment time increases (Fig. 2A). The SH content decreased from 0.56 nmol/mg protein (control sample) to 0.34 nmol/mg protein after being treated with ACP for 300 s. It has been also found that the decrease of SH content is treatment time-dependent (Fig. 2A). The most likely explanation of the decline of SH content is that the generated plasma reactive species, lead to either strong oxidation of the side chains of sulfur-containing protein or aggregation of disulfide bonds through cross-linking of sulfhydryl groups in the sulfur amino acids such as methionine and cysteine (Tolouie, Mohammadifar, Ghomi, & Hashemi, 2018). The reduction of SH content indicates the loss of most reactive SH functional groups, which are essential in protein folding and stability (Segat et al., 2015).

In order to quantify the oxidation of crude protease extract, the amount of protein-bound carbonyl groups was examined, the results for

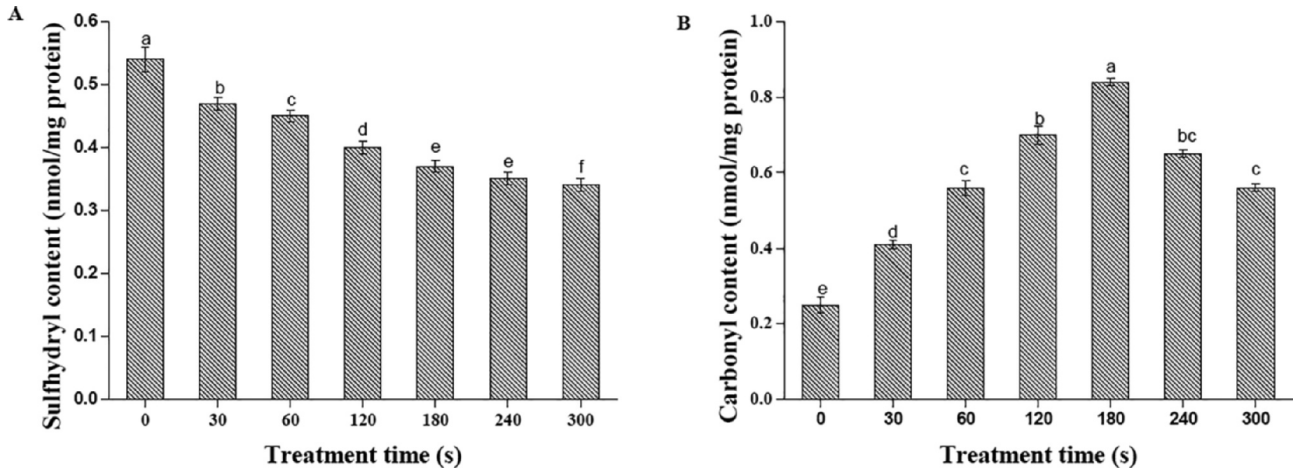

Fig. 2. Effect of atmospheric cold plasma (ACP) on sulfhydryl content (A) and Carbonyl content (B) of hairtail crude protease extract. Different letters on top of bars indicate a statistically significant difference at $p < 0.05$. Values represent the means of triplicate measurements ± standard deviation (n = 3). 0 s refers to the untreated sample (control).

which are given in Fig. 2B. The protein carbonyl content has been increased after treatment with ACP. The untreated control CPE sample contained about 0.23 nmol carbonyl/mg protein, which was increased to 0.9 nmol carbonyl/mg protein ($p < 0.05$) when the ACP treatment was conducted for 180 s. After 300 s of ACP treatment, a significant decreased of carbonyl content to 0.7 nmol carbonyl/mg protein was found (Fig. 2B). These findings indicated that the chemical modification of crude protease extract strongly depended on plasma species exposure time. ACP treatment caused protein chemical modification and generation of carbonyl derivative in the sample that resulted in changes in the carbonyl content (Zhang et al., 2013) this, in turn, leads to loss functions of the protein. More specifically, the fragmentation of protein backbone through α-amidation and β-scission as well as direct or indirect oxidation of amino acids side chains including proline, arginine, lysine, and threonine, lead to the formation of carbonyl derivatives (Chen et al., 2015). A similar effect was documented for proteolytic enzymes from squid mantle (Nyaisaba et al., 2019).

3.5. Effect of ACP on protein solubility and turbidity

Protein Solubility could be used as an indirect indication of protein oxidation and denaturation since the oxidation and denaturation of proteins usually followed by a decrease in protein solubility due to protein aggregation and formation of insoluble condensate (Joo, Kauffman, Kim, & Park, 1999). ACP significantly ($p < 0.05$) affected the solubility and turbidity of total protein as shown in Fig. 3 (A and B) respectively. Compared to control samples, samples treated by ACP showed lower solubility in total proteins with increasing treatment time ($p < 0.05$). The lowest solubility percentage (47%) was observed at the treatment time of 180 s (Fig. 3A). The decrease in solubility with increased treatment time, probably due to the denaturation and aggregation of the protein molecules after exposed to plasma active species (Benjakul et al., 2000). These results correspond with Nyaisaba et al. (2019) who found that the ACP treatment strongly reduce the protein solubility by 63.58% after 180 s (Nyaisaba et al., 2019).

The changes in the turbidity levels were used to observe hairtail protein aggregation. As expected, a significant increase ($p < 0.05$) in turbidity with an increased ACP treatment time is observed (Fig. 3B). The maximum turbidity of 0.47 (at A350 nm) was obtained after 120 s of ACP treatment. Afterward, a decrease in turbidity was observed from 180 s to 300 s treatment times, however, the turbidity level in the treated samples kept higher than the control samples. The increase in the turbidity resulted from the aggregation of protein concentrates, which trigger the formation of insoluble aggregates by polymerization of monomer protein into larger protein (Ekezie et al., 2019; Li et al., 2013).

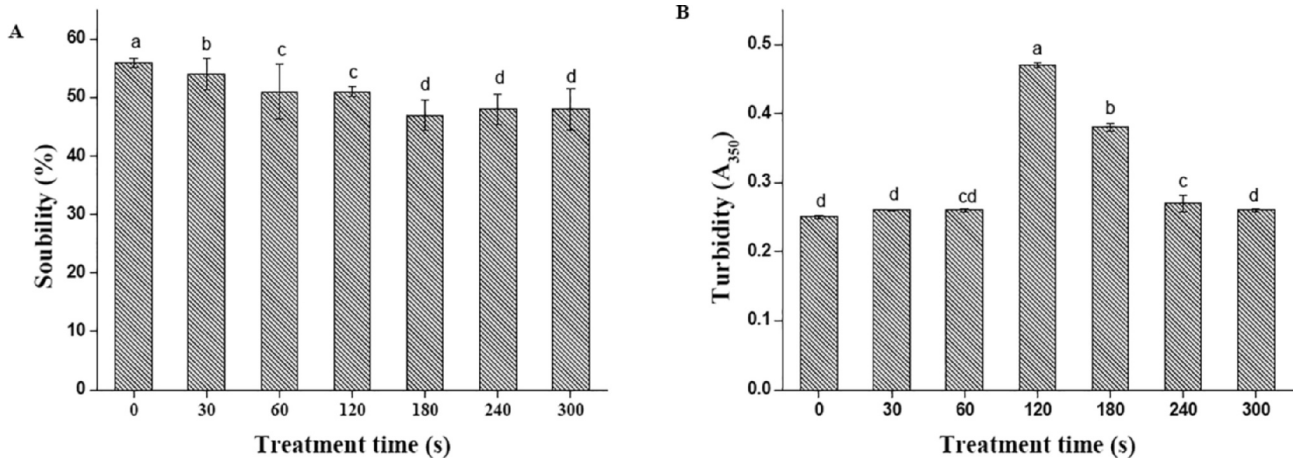

Fig. 3. Effect of atmospheric cold plasma (ACP) on solubility (A) and turbidity (B) of muscle protein of hairtail. Different letters on the top of the bars indicate a statistically significant difference at $p < 0.05$. Values represent the means of triplicate measurements ± standard deviation (n = 3). 0 s refers to the untreated sample (control).

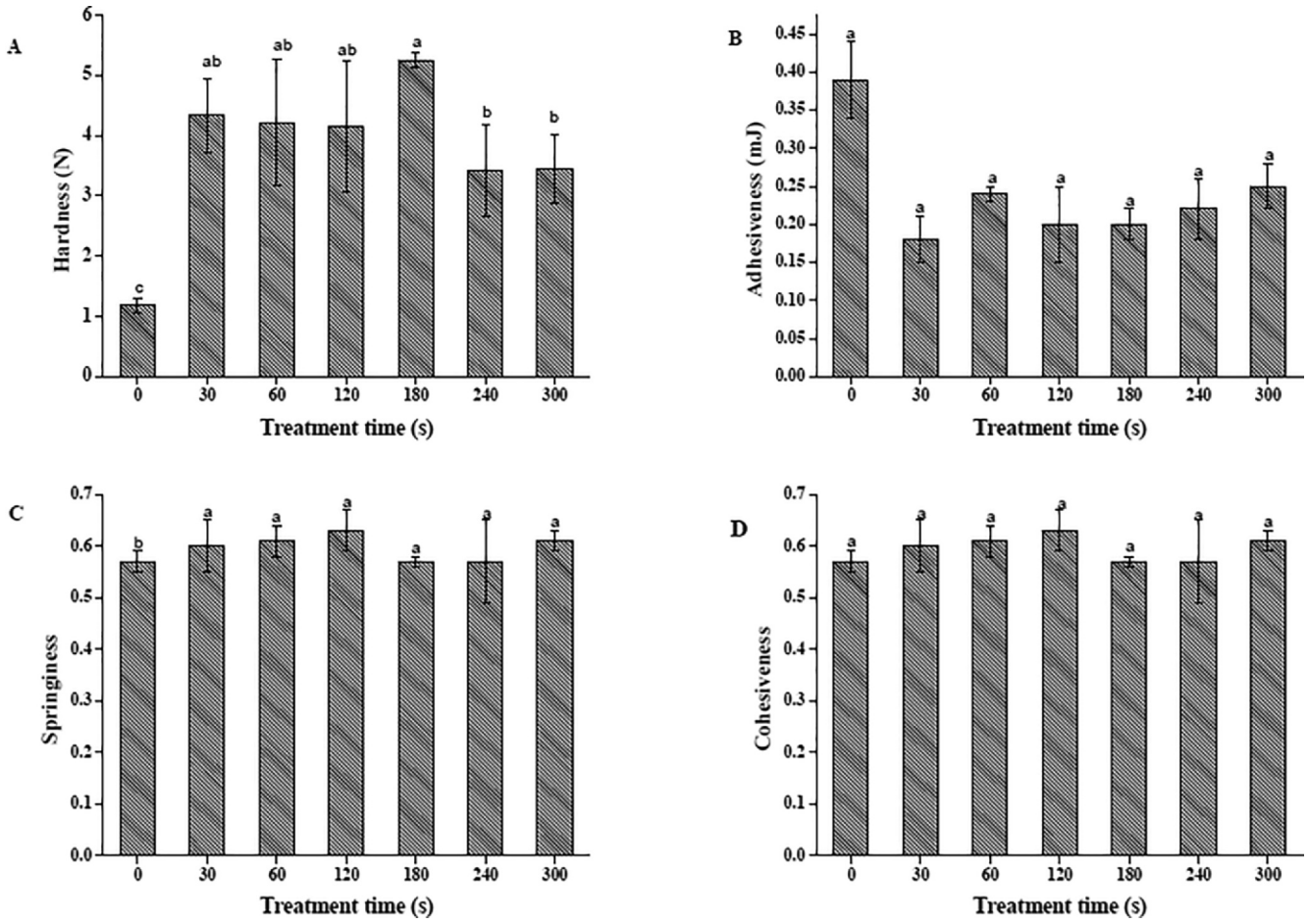

Fig. 4. Effect of atmospheric cold plasma (ACP) on TPA of hairtail muscle protein. Hardness (A), Adhesiveness (B), Springiness (C), and Cohesiveness (D). Different letters on the top of the bars indicate a statistically significant difference at $p < 0.05$. Values represent the means of triplicate measurements ± standard deviation (n = 3). 0 s refers to the untreated sample (control).

Table 1
Effect of atmospheric plasma on color and water holding capacity of hairtail muscle protein.

Treatment time (s)	Color			Water holding capacity (%)
	L*	a*	b*	
0	75.77 ± 0.12^{c}	−1.51 ± 0.04^{a}	10.12 ± 0.02^{e}	61.12 ± 1.70^{b}
30	74.50 ± 0.24^{d}	−1.66 ± 0.07^{a}	10.20 ± 0.24^{e}	74.69 ± 4.06^{a}
60	75.76 ± 0.08^{c}	−1.81 ± 0.11^{a}	10.68 ± 0.29^{ec}	75.43 ± 2.13^{a}
120	72.65 ± 0.24^{e}	−1.53 ± 0.36^{a}	10.40 ± 0.09^{de}	67.81 ± 3.30^{ab}
180	77.49 ± 0.27^{b}	−1.73 ± 0.10^{a}	11.25 ± 0.28^{b}	68.39 ± 4.53^{ab}
240	77.47 ± 0.25^{b}	−1.63 ± 0.13^{a}	12.21 ± 0.32^{a}	65.81 ± 5.32^{b}
300	79.12 ± 0.08^{a}	−1.67 ± 0.09^{a}	11.00 ± 0.06^{bc}	62.99 ± 2.09^{b}

Results are presented as mean ± standard deviation (n = 3). Different subscript letters on values within a column represent a significant difference ($p < 0.05$). 0 s refers to the ACP untreated sample (control).

3.6. Effect of ACP on texture profile of hairtail muscle

Assessment of the ACP effect on the general texture profiles of hairtail muscle protein was conducted using Texture Profile Analysis (TPA). As given in Fig. 4 (A - D), the determination of TPA involved four parameters namely: hardness, springiness, cohesiveness, and adhesiveness. As a general trend, the texture profile of the hairtail muscle treated with ACP had better textural properties compared to the untreated samples. Fig. 4A shows that the samples treated with ACP had the highest hardness (5.25 N) after 180 s of treatment compared to the control sample which had a hardness of 1.18 N. Fish hardness is possibly correlated to its muscle fibers (Luan et al., 2018). These results in a good agreement with Nyaisaba et al. (2019) who found that the hardness of squid gel increased after ACP treatment at 60 kV (Nyaisaba et al., 2019). After ACP treatment, adhesiveness decreased from 0.39 mJ in the control sample to 0.18 mJ after 30 s (Fig. 4B). With increasing the treatment time, the adhesiveness increased gradually, however, it stayed lower than the control sample. The springiness and cohesiveness (Fig. 4C and 5D) showed an increasing trend similar to hardness as treating time increased. The TPA results provide evidence that ACP treatment exposes hairtail muscle protein to oxidation causing cross-linking and denser protein networks which in turn results in better texture properties.

3.7. Effect of ACP on water holding capacity (WHC) and color of hairtail muscle

The ability of ACP to enhance the unfolding of polysaccharide chain and proteins is reported to increase the number of water molecules that can bond with proteins and polysaccharides (Ji, Xue, Zhang, Li, & Xue, 2017). Table 1 shows a significant increase ($p < 0.05$) in WHC of hairtail muscle protein from 61.12% in the control sample to 75.43% after 60 s of ACP treatment. The WHC for muscle protein has been improved where more water was entrapped in the three-dimensional network structure, this could be because of the capability of plasma species to induce aggregation reactions (Chanarat & Benjakul, 2013). It is worth to mention that a slight decrease in WHC has been observed with extending the treatment time to reach to the lowest value of 62.99% after 300 s. However, the lowest value obtained in samples treated with ACP was higher than the WHC recorded in the control samples. This decrease would be attributed to the damage which could occur in the protein molecules as the exposure time to plasma active species increased (Huda, Leng, & Nopiant, 2011). The higher water holding capacity in the ACP treated samples observed in this study concurs to the findings conducted by Fu et al. (2012).

For the impact of ACP on the color of the hairtail muscle Table 1 shows that there is a significant increase ($p < 0.05$) in lightness (L*) of the treated samples compared to the control sample. The lightness values of treated samples were higher than that of control samples, the increase in L* values was found to be treatment time-dependent. (Park, 1995) indicated that the increase in water-holding capacity induced by ACP treatment could be the main reason for the improvement of hairtail protein color. Similar outcomes have been concluded by Lin, Yang, Xu, Jie, and Liu (2015)) who observed that electron irradiation treatment enhances the lightness of the hairtail muscle. On the other hand, an irregular trend was observed in other color parameters such as a* (redness/greenness) and b* (yellowness/blueness).

3.8. SDS – PAGE patterns

To investigate the effect of ACP treatment on the structure of hairtail protein SDS – PAGE analysis was conducted. Generally, ACP induces covalent linkages between protein molecules and protein fragments formation. Fig. 5 shows that no change has been observed in the number of protein bands in the samples treated with ACP compared with the untreated sample (control). Studies conducted to investigate the effect of irradiation on Atlantic salmon (Yang et al., 2014), and myofibril proteins from hairtail (Lin et al., 2015) indicated similar findings and pointed out a slight effect of irradiation on the molecular weight of different protein bands. The high strength of myosin heavy chains (MHC) and actin indicates these molecules to be the main protein constituents in hairtail protein. Besides, the protein patterns show a significant increase in band intensity of MHC and Actin when the ACP treatment time increased to 120 s; 180 s; 240 s; and 300 s, that could be due to protein structural change involving covalent linkages in proteins, the formation of fragments as a result of cross-linking, and aggregation caused by protein oxidation (Zhang et al., 2018). The exposure of the protein to plasma species for a long time causes variations on the degree of cross-linking of myosin heavy chain leading to variation in the strength of band intensity (Nyaisaba et al., 2019; Zhang et al., 2018). (Lopez-Enriquez, Ocano-Higuera, Torres-Arreola, Ezquerra-Brauer, & Marquez-Rios, 2015) studied the effect of ACP on sarcoplasmic proteins from giant squid (*Dosidicus gigas*) mantle, the results detected a mild increase in protein band intensity below 25 kDa molecular, which resulted in changes in the activity of the endogenous enzymes.

4. Conclusion

The available information regarding the impact on ACP on the quality of the hairtail muscle protein is insufficient, as well limited researches exist on the influence of ACP on crude protease extract and its relation with improving the quality of the hairtail muscle protein. In this study, the effect of ACP at 50 kV and with different treatment times on the crude protease extract and muscle protein from hairtail fish has been investigated. The results concluded that implementing ACP at 50 kV was able to inhibit the activity of crude protease extract to the lowest value of 0.035 units/mg protein after 240 s. Protein oxidation indices (carbonyls and sulfhydryl) vary significantly when crude protease enzyme was exposed to plasma active species. An enhancement in the color and water holding capacity properties has been observed in hairtail samples treated with ACP. Therefore, ACP treatment could be used as an effective non-thermal method to maintain the quality of hairtail fish and extend the shelf-life. Supplementary research is needed to provide knowledge concerning the effect of ACP treatment on the lipid oxidation of hairtail muscle.

CRediT authorship contribution statement

John Kilian Koddy: Data curation, Formal analysis, and Investigation, Methodology. **Wenhua Miao:** Conceptualization, Project administration, Supervision, Validation, Visualization, Resources. **Shaimaa Hatab:** Conceptualization, Project administration, Supervision, Validation, Visualization, Resources, Writing - review & editing. **Lingling Tang:** Data curation, Formal analysis. **Huiqian Xu:**

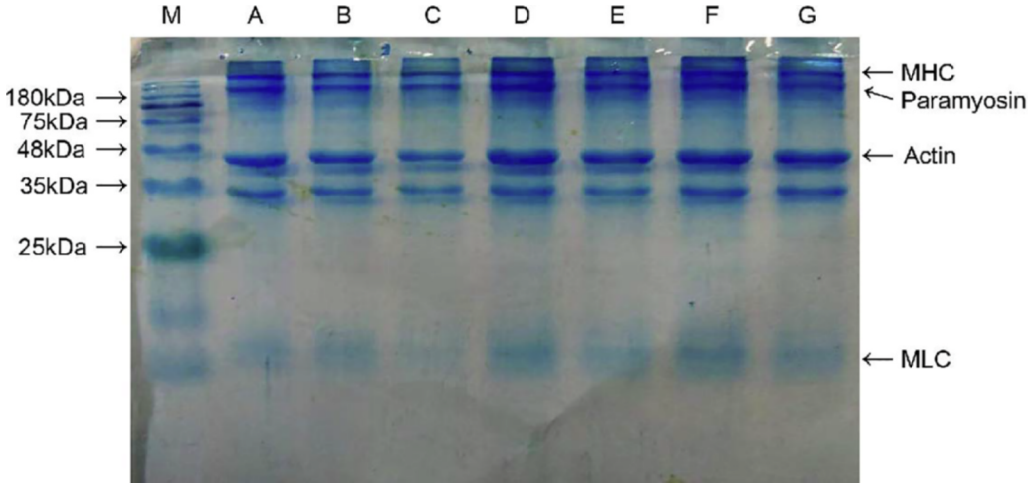

Fig. 5. The protein patterns of hairtail muscle with and without ACP treatments. M- marker, A- untreated sample; B- 30 s; C- 60 s; D- 120 s; E- 180 s; F- 240 s; G- 300 s.

Investigation, Methodology. **Bhoke Marwa Nyaisaba:** Software, Writing - original draft. **Meiling Chen:** Supervision, Validation, Visualization. **Shanggui Deng:** Supervision, Validation, Visualization, Project administration.

Declaration of Competing Interest

The authors declare that they have no known competing financial interests or personal relationships that could have appeared to influence the work reported in this paper.

Acknowledgments

This work was supported by the Zhejiang Provincial Public Technology Research Program [LGJ20C200002], and the University Student Science and Technology Innovation Activity Plan and New Talet Plan Project of Zhejiang Province (2018R411050).

Compliance with ethics requirements

This work does not include data collection from animal or human subjects.

Appendix A. Supplementary data

Supplementary data to this article can be found online at https://doi.org/10.1016/j.foodchem.2020.128418.

References

Benjakul, S., & Visessanguan, W. (2003). Transglutaminase-mediated setting in bigeye snapper Surimi. *Food Research International, 36*(3), 253–266.

Benjakul, S., Visessanguan, W., Tanaka, M., Ishizaki, S., Taluengphol, A., & Chichanan, U. (2000). Physicochemical and textural properties of dried squid as affected by alkaline treatments. *Journal of the Science of Food and Agriculture, 80*(14), 2142–2148.

Chanarat, S., & Benjakul, S. (2013). Impact of microbial transglutaminase on gelling properties of Indian mackerel fish protein isolates. *Food Chemistry, 136*(2), 929–937.

Chen, L., Zhou, G., & Zhang, W. (2015). Effects of high oxygen packaging on tenderness and water holding capacity of pork through protein oxidation. *Food and Bioprocess Technology, 8*(11), 2287–2297.

Cheng, Q., & Sun, D. W. (2008). Factors affecting the water holding capacity of red meat products: A review of recent research advances. *Critical Reviews in Food Science and Nutrition, 48*(2), 137–159.

Ekezie, F.-G.-C., Cheng, J.-H., & Sun, D. (2019). Effects of atmospheric pressure plasma jet on the conformation and physicochemical properties of myofibrillar proteins from king prawn (*Litopenaeus vannamei*). *Food Chemistry, 276*, 147–156.

Fernández, K., Aspé, E., & Roeckel, M. (2010). Scaling up parameters for shelf-life extension of Atlantic Salmon (*Salmo salar*) fillets using superchilling and modified atmosphere packaging. *Food Control, 21*(6), 857–862.

Fu, X., Hayat, K., Li, Z., Lin, Q., Xu, S., & Wang, S. (2012). Effect of microwave heating on the low-salt gel from silver carp (*Hypophthalmichthys molitrix*) surimi. *Food Hydrocolloids, 27*(2), 301–308.

Gavahian, M., Chu, Y.-H., & Jo, C. (2019). Prospective applications of cold plasma for processing poultry products: Benefits, effects on quality attributes, and limitations. *Comprehensive Reviews in Food Science and Food Safety, 18*(4), 1292–1309.

Gómez-Guillén, M. C., Hurtado, J. L., & Montero, P. (2002). Autolysis and protease inhibition effects on dynamic viscoelastic properties during thermal gelation of squid muscle. *Journal of Food Science, 67*(7), 2491–2496.

Graves, D. B. (2014). Reactive species from cold atmospheric plasma: Implications for cancer therapy. *Plasma Processes and Polymers, 11*(12), 1120–1127.

Huda, N., Leng, O. H., & Nopiant, R. (2011). Fisheries and aquatic science. *Journal of Fisheries and Aquatic Science, 6*(4), 404–416.

Ji, L., Xue, Y., Zhang, T., Li, Z., & Xue, C. (2017). The effects of microwave processing on the structure and various quality parameters of Alaska pollock surimi protein-polysaccharide gels. *Food Hydrocolloids, 63*, 77–84.

Joo, S. T., Kauffman, R. G., Kim, B. C., & Park, G. B. (1999). The relationship of sarcoplasmic and myofibrillar protein solubility to colour and water-holding capacity in porcine longissimus muscle. *Meat Science, 52*(3), 291–297.

Ketnawa, S., Martinez-Alvarez, O., Benjakul, S., & Rawdkuen, S. (2015). Extraction and biochemical characterization of peptidases from giant catfish viscera by aqueous two-phase system. *Journal of Food Biochemistry, 39*(4), 429–438.

Klomklao, S., Benjakul, S., Kishimura, H., & Chaijan, M. (2011). Extraction, purification, and properties of trypsin inhibitor from Thai mung bean (*Vigna radiata* (L.) R. Wilczek). *Food Chemistry, 129*(4), 1348–1354.

Konno, K., & Fukazawa, C. (1993). Autolysis of squid mantle muscle protein as affected by storage conditions and inhibitors. *Journal of Food Science, 58*(6), 1198–1202.

Li, Y., Kong, B., Xia, X., Liu, Q., & Diao, X. (2013). Structural changes of the myofibrillar proteins in common carp (*Cyprinus carpio*) muscle exposed to a hydroxyl radical-generating system. *Process Biochemistry, 48*(5), 863–870.

Lin, X., Yang, W., Xu, D., Jie, Z., & Liu, W. (2015). Improving gel properties of hairtail surimi by electron irradiation. *Radiation Physics and Chemistry, 110*, 1–5.

Lopez-Enriquez, R. L., Ocano-Higuera, V. M., Torres-Arreola, W., Ezquerra-Brauer, J. M., & Marquez-Rios, E. (2015). Chemical and functional characterization of sarcoplasmic proteins from giant squid (*Dosidicus gigas*) mantle. *Journal of Chemistry, 2015*, Article 538721.

Luan, L., Fu, S., Yuan, C., Ishimura, G., Chen, S., Chen, J., & Hu, Y. (2017). Combined effect of superchilling and tea polyphenols on the preservation quality of hairtail (*Trichiurus haumela*). *International Journal of Food Properties, 20*, S992–S1001.

Luan, L., Sun, Y., Chen, S., Wu, C., & Hu, Y. (2018). A study of fractal dimension as a quality indicator of hairtail (*Trichiurus haumela*) samples during frozen storage. *Scientific Reports, 8*(1), 16468.

Miao, W., Nyaisaba, B. M., Koddy, J. K., Chen, M., Hatab, S., & Deng, S. (2020). Effect of cold atmospheric plasma on the physicochemical and functional properties of myofibrillar protein from Alaska pollock (*Theragra chalcogramma*). *International Journal of Food Science & Technology, 55*(2), 517–525.

Nyaisaba, B. M., Liu, X., Zhu, S., Fan, X., Sun, L., Hatab, S., ... Deng, S. (2019). Effect of hydroxyl-radical on the biochemical properties and structure of myofibrillar protein from Alaska pollock (*Theragra chalcogramma*). *LWT -Food Science and Technology, 106*, 15–21.

Nyaisaba, B. M., Miao, W., Hatab, S., Siloam, A., Chen, M., & Deng, S. (2019). Effects of cold atmospheric plasma on squid proteases and gel properties of protein concentrate from squid (*Argentinus ilex*) mantle. *Food Chemistry, 291*, 68–76.

Pankaj, S., Misra, N. N., & Cullen, P. J. (2013). Kinetics of tomato peroxidase inactivation by atmospheric pressure cold plasma based on dielectric barrier discharge. *Innovative Food Science & Emerging Technologies, 19*, 153–157.

Pankaj, S., Wan, Z., & Keener, K. (2018). Effects of cold plasma on food quality: A Review. *Foods (Basel, Switzerland), 7*(1), 4.

Park, J. W. (1995). Surimi gel colors as affected by moisture content and physical conditions. *Journal of Food Science, 60*(1), 15–18.

Segat, A., Misra, N. N., Cullen, P. J., & Innocente, N. (2015). Atmospheric pressure cold plasma (ACP) treatment of whey protein isolate model solution. *Innovative Food Science & Emerging Technologies, 29*, 247–254.

Segat, A., Misra, N. N., Cullen, P. J., & Innocente, N. (2016). Effect of atmospheric pressure cold plasma (ACP) on activity and structure of alkaline phosphatase. *Food and Bioproducts Processing, 98*, 181–188.

Shavandi, A., Hou, Y., Carne, A., McConnell, M., & Bekhit, A. E.-d. A. (2019). Chapter four - marine waste utilization as a source of functional and health compounds. In F. Toldrá (Ed.), Advances in Food and Nutrition Research, vol. 87 (187-254): Academic Press.

Singh, A., & Benjakul, S. (2018). Proteolysis and its control using protease inhibitors in fish and fish products: A Review. *Comprehensive Reviews in Food Science and Food Safety, 17*(2), 496–509.

Stadtman, E. R. (2006). Protein oxidation and aging. *Free Radical Research, 40*(12), 1250–1258.

Tappi, S., Berardinelli, A., Ragni, L., Dalla Rosa, M., Guarnieri, A., & Rocculi, P. (2014). Atmospheric gas plasma treatment of fresh-cut apples. *Innovative Food Science & Emerging Technologies, 21*, 114–122.

Tolouie, H., Mohammadifar, M. A., Ghomi, H., & Hashemi, M. (2018). Cold atmospheric plasma manipulation of proteins in food systems. *Critical reviews in food science and nutrition, 58*(15), 2583–2597.

Yang, Z., Wang, H., Wang, W., Qi, W., Yue, L., & Ye, Q. (2014). Effect of 10 MeV E-beam irradiation combined with vacuum-packaging on the shelf life of Atlantic salmon fillets during storage at 4 °C. *Food Chemistry, 145*, 535–541.

Zhang, H., Ma, J., Shen, J., Lan, Y., Ding, L., Qian, S., ... Chu, P. K. (2018). Comparison of the effects induced by plasma generated reactive species and H_2O_2 on lactate dehydrogenase (LDH) enzyme. *IEEE Transactions on Plasma Science, 46*(8), 2742–2752.

Zhang, H., Xu, Z., Shen, J., Li, X., Ding, L., Ma, J., ... Chu, P. K. (2015). Effects and mechanism of atmospheric-pressure dielectric barrier discharge cold plasmaon lactate dehydrogenase (LDH) enzyme. *Scientific Reports, 5*(1), 10031.

Zhang, T., Xue, Y., Li, Z., Wang, Y., & Xue, C. (2015). Effects of deacetylation of konjac glucomannan on Alaska Pollock surimi gels subjected to high-temperature (120°C) treatment. *Food Hydrocolloids, 43*, 125–131.

Zhang, W., Xiao, S., & Ahn, D. U. (2013). Protein oxidation: Basic principles and implications for meat quality. *Critical Reviews in Food Science and Nutrition, 53*, 1191–1201.